

# Geophysical Research Letters



## RESEARCH LETTER

10.1029/2020GL090700

### Key Points:

- We present the first statistical analysis of emissions at 180–230, 337, and 777 nm coincident with TGFs as measured by a single platform
- 90% of TGFs occur at the onset of large-amplitude optical pulses supporting the streamer-leader mechanism for TGF generation
- The sources of the emissions are estimated to be 1–5 km below the cloud tops

### Supporting Information:

- Supporting Information S1

### Correspondence to:

M. Heumesser,  
[heumat@space.dtu.dk](mailto:heumat@space.dtu.dk)

### Citation:

Heumesser, M., Chanrion, O., Neubert, T., Christian, H. J., Dimitriadou, K., Gordillo-Vazquez, F. J., et al. (2021). Spectral observations of optical emissions associated with Terrestrial Gamma-Ray Flashes. *Geophysical Research Letters*, 48, e2020GL090700. <https://doi.org/10.1029/2020GL090700>

Received 7 SEP 2020  
Accepted 17 DEC 2020

## Spectral Observations of Optical Emissions Associated With Terrestrial Gamma-Ray Flashes

Matthias Heumesser<sup>1</sup> , Olivier Chanrion<sup>1</sup> , Torsten Neubert<sup>1</sup> , Hugh J. Christian<sup>2</sup>, Krystallia Dimitriadou<sup>1</sup> , Francisco J. Gordillo-Vazquez<sup>3</sup> , Alejandro Luque<sup>3</sup> , Francisco Javier Pérez-Invernón<sup>3,4</sup> , Richard J. Blakeslee<sup>5</sup> , Nikolai Østgaard<sup>6</sup> , Victor Reglero<sup>7</sup>, and Christoph Köhn<sup>1</sup> 

<sup>1</sup>National Space Institute, Technical University of Denmark (DTU Space), Kongens Lyngby, Denmark, <sup>2</sup>Department of Atmospheric Science, Earth System Science Center, University of Alabama in Huntsville, Huntsville, AL, USA, <sup>3</sup>Instituto de Astrofísica de Andalucía (IAA, CSIC), Granada, Spain, <sup>4</sup>Institut für Physik der Atmosphäre, Deutsches Zentrum für Luft- und Raumfahrt (DLR), Oberpfaffenhofen, Germany, <sup>5</sup>NASA Marshall Space Flight Center, Huntsville, AL, USA, <sup>6</sup>Birkeland Centre for Space Science, University of Bergen, Bergen, Norway, <sup>7</sup>Image Processing Laboratory, University of Valencia, Valencia, Spain

**Abstract** The Atmosphere-Space Interactions Monitor measures Terrestrial Gamma-Ray Flashes (TGFs) simultaneously with optical emissions from associated lightning activity. We analyzed optical measurements at 180–230, 337, and 777.4 nm related to 69 TGFs observed between June 2018 and October 2019. All TGFs are associated with optical emissions and 90% of them are at the onset of a large optical pulse, suggesting that they are connected with the initiation of current surges. A model of photon delay induced by cloud scattering suggests that the sources of the optical pulses are from 0.7 ms before to 4.4 ms after the TGFs, with a median of  $-10 \pm 80 \mu\text{s}$ , and 1–5 km below the cloud top. The pulses have rise times comparable to lightning but longer durations. Pulse amplitudes at 337 nm are  $\sim 3$  times larger than at 777.4 nm. The results support the leader-streamer mechanism for TGF generation.

**Plain Language Summary** Terrestrial Gamma-Ray Flashes (TGFs) are short bursts of high-energy radiation produced in thunderstorms, first observed from astrophysical spacecraft during the 1990s. This study characterizes optical emissions from lightning associated with these flashes in multiple wavelengths to help finding their production mechanism. The data are collected by space based instruments aboard the International Space Station as it passes over the major thunderstorm regions of the Earth. We find that TGFs are associated with propagation of intracloud lightning in the upper cloud levels. With the help of a model of light propagation through a cloud, we estimate the source of the respective optical emissions to be 1–5 km below the cloud tops. By investigating TGFs and their connection to lightning, we can understand the energy and timescales of lightning better, eventually leading to a better understanding of cloud physics and thunderstorms in general.

## 1. Introduction

Terrestrial Gamma-Ray Flashes (TGFs) are bursts of X-rays and gamma-rays from thunderstorms (Fishman et al., 1994). They are bremsstrahlung from relativistic runaway electrons, powered by the electric fields within the thunderstorm clouds (Gurevich et al., 1992; Wilson, 1925). These bursts last between 10 and a few 100  $\mu\text{s}$  (Marisaldi et al., 2014; Østgaard et al., 2019b) with detected photon energies of up to 40 MeV (Marisaldi et al., 2019). To explain the observed photon fluxes, one model considers the amplification of the electron flux in impulsive, 10–100 meter-scale, intense electric fields at the tip of lightning leaders (Celestin & Pasko, 2011; Chanrion et al., 2014; da Silva & Pasko, 2013; Köhn & Ebert, 2015; Moss et al., 2006; Xu et al., 2012). In this scenario, TGFs would always be associated with optical radiation from leaders. In another model, the electron flux is created by the kilometer-scale electric fields within the clouds via backscattered X-rays and inversely propagating positrons, created by pair production, to seed additional avalanches. This feedback mechanism suggests the TGF production to be associated with modest levels of optical emissions if it is acting alone (Dwyer, 2008). However, the two mechanisms do not exclude each other as the region around leader tips can locally facilitate the feedback mechanism (Köhn et al., 2017). Optical meas-

© 2020. The Authors.

This is an open access article under the terms of the [Creative Commons Attribution-NonCommercial-NoDerivs](https://creativecommons.org/licenses/by-nc-nd/4.0/) License, which permits use and distribution in any medium, provided the original work is properly cited, the use is non-commercial and no modifications or adaptations are made.

measurements, as those presented in the following, can help to identify the mechanism that generates relativistic electrons as discussed by Xu et al. (2015).

Recent observations have shown that TGFs occur at the onset of optical emissions, which point to the importance of lightning leaders (Neubert et al., 2020; Østgaard et al., 2019b). The measurements were obtained by the Atmosphere-Space Interactions Monitor (ASIM) on the International Space Station (ISS) carrying sensors in selected bands in the range from the infra-red to gamma-ray energies. With sensors on a common platform, ambiguities in the relative timing of the sensor data are reduced, a problem that has followed past studies attempting to correlate data from different satellites or on the ground (Alnussirat et al., 2019; Gjesteland et al., 2017; Østgaard et al., 2013).

In the present study, we analyze the UV and optical emissions detected by ASIM in connection with TGFs, measurements that have not been obtained in this detail before. We characterize the emissions relative to the TGF onset time, relate them to lightning propagation scenarios, and estimate their depth within the clouds. Section 2 gives an overview of the ASIM instruments, the data and the analysis methods; Section 3 presents the results and Section 4 presents a discussion.

## 2. Measurements and Analysis

ASIM on the ISS is designed to observe lightning, TGFs, and Transient Luminous Events (TLEs; Neubert et al., 2019) and consists of the Modular Multispectral Imaging Array (MMIA) and the Modular X-ray and Gamma-ray Sensor (MXGS), both pointing toward nadir. The MXGS has a high-energy detector ( $\sim 0.3$  to  $>30$  MeV) that measures day and night with a time resolution of 28.7 ns and a low-energy detector ( $\sim 50$ – $400$  keV) that measures with a time resolution of  $1 \mu\text{s}$ , but only during the night because of optical photon contamination (Østgaard et al., 2019a). The MMIA includes three photometers and two cameras with the same field of view. The photometers sample at 100 kHz at 180–230 nm (UV), which includes part of the  $\text{N}_2$  Lyman-Birge-Hopfield lines, at 337/4 nm (blue; center of band/bandwidth) that includes the strongest line of  $\text{N}_2\text{P}$ , and at 777.4/5 nm (red), an atomic oxygen line considered one of the strongest emission lines of the lightning spectrum. The cameras capture 12 frames per second at 337/4 nm and 777.4/3 nm with  $\sim 400 \times 400$  m ground resolution at nadir (Chanrion et al., 2019). The MMIA is only operational during night to prevent damage by sunlight. The instrument computers include flash trigger logic that saves all sensor data if one sensor detects a flash.

In the period extending from the end of the commissioning phase on June 2, 2018 to October 26, 2019, ASIM observed 69 TGFs during the night inside the field of view (FOV) of the MMIA, all associated with optical emissions. The selected events were not associated with activity outside the MMIA FOV but inside the larger FOV of the Lightning Imaging Sensor on the ISS (ISS-LIS), rectangular with a diagonal of 1,000 km (Blakeslee et al., 2020), or the global lightning detection network GLD360 network in a box of  $\pm 6^\circ$  latitude and longitude; both within a 200 ms window centered at the TGF time. The likelihood that the TGF events are associated with lightning activity not observed by the MMIA is then reduced. During the first 10 months of nominal operation, the relative timing uncertainty between the MXGS and MMIA was up to  $\pm 80 \mu\text{s}$ , improving to  $\pm 5 \mu\text{s}$  after a software update in April 2019 (Østgaard et al., 2019b). The absolute time accuracy is better than 25 ms, but can often be improved to  $\sim 1$  ms by correlation with ground-based lightning detection data from, for instance, GLD360 and data from ISS-LIS. Such corrective improvement was possible for nearly 90% of the cases considered here.

Three examples of the optical signals measured by the photometers are shown in Figure 1. In all cases, the TGFs are preceded by lower level preactivity and are followed by high amplitude emissions. In the less common case (Figure 1a), the TGFs are followed by few pulses, but more often they are followed by a longer sequence of pulses (Figures 1c and 1e). In the analysis, we focus on a  $\pm 20$  ms time interval around the TGFs that includes the lower level activity prior to a TGF and the pulses that follow immediately after, but excludes continued, longer-duration activity after a TGF.

Preactivity is estimated from signal increases over the background noise level occurring before the TGF and originating from a single cloud top region, verified at 2 ms/4 km resolution by ISS-LIS. The MMIA instrument stores data (1 frame, 83 ms) before a triggering event to include the present background (Chanrion

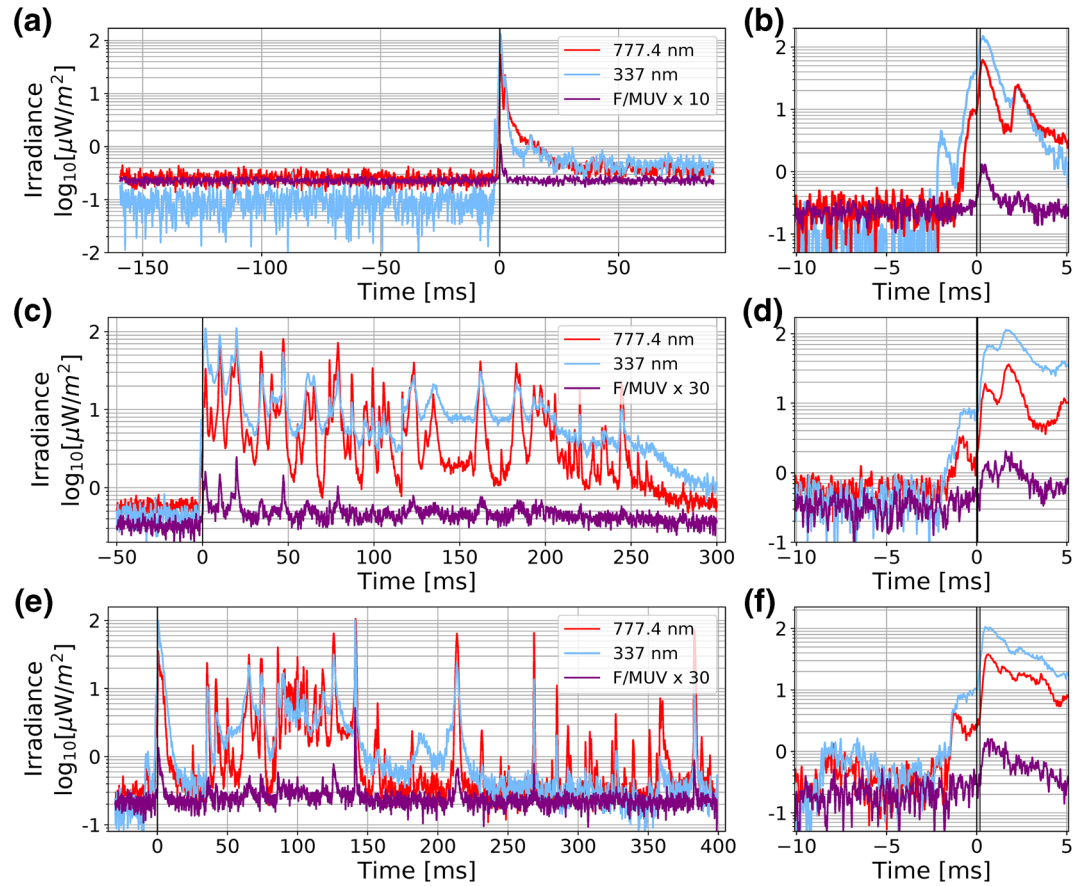


**Figure 1.** Typical optical signals observed in relation to Terrestrial Gamma-Ray Flashes (TGFs). Time is relative to the detection of the first TGF photon (vertical black line) on May 26, 2019, 02:29:34.993 (a), (b); July 28, 2018, 17:03:15.848 (c), (d); and September 1, 2018, 06:52:55.294 (e), (f). The signal is 10-point (a,c,e) and 2-point (b,d,f), Gaussian filtered.

et al., 2019), allowing us to take the average irradiance of the first 80–100 ms of an observation plus twice the standard deviation as noise level. The procedure is done for the three wavelengths independently, but no standard deviation is added in the UV band. Start and end of the preactivity pulses are the moments when the signal crosses the noise level and the respective intensity is the pulse maximum. Modest levels of preactivity are  $\leq 15\%$  of the main peak maximum, high levels are  $> 15\%$ .

The optical signals are affected by photon scattering and absorption by cloud particles, which determine the shape of the recorded light curve (Koshak et al., 1994; Light et al., 2001; Thomason & Krider, 1982). To estimate scattering effects, we apply a new, physical approach offered by Soler et al. (2020) and Luque et al. (2020). They present a model of an instantaneous, point-like source inside a planar, homogeneous cloud, where the normalized function describing the pulse shape observed above a cloud is

$$f(t, t_0, \tau, \nu) = \sqrt{\frac{\tau}{\pi(t-t_0)^3}} \exp\left(2\sqrt{\nu\tau} - \frac{\tau}{(t-t_0)} - \nu(t-t_0)\right); t > t_0 \quad (1)$$

where  $t$  is time,  $t_0$  is the *source time* when the source releases photons,  $\tau$  is the characteristic diffusion time and  $\nu$  is the absorption rate. For those TGF events that are associated with a simple optical pulse, we subtract the noise level before scaling and fitting the function to the pulse. The fitting procedure is illustrated in Figure 2 for the cases of modest prepulse activity (a) and high prepulse activity (b). Higher prepulse activity increases the uncertainties of the three fitting parameters, as discussed later. We use the fitted function to define the times  $t_x$  where the pulses reach  $x\%$  of their signal maximum and derive parameters such as the

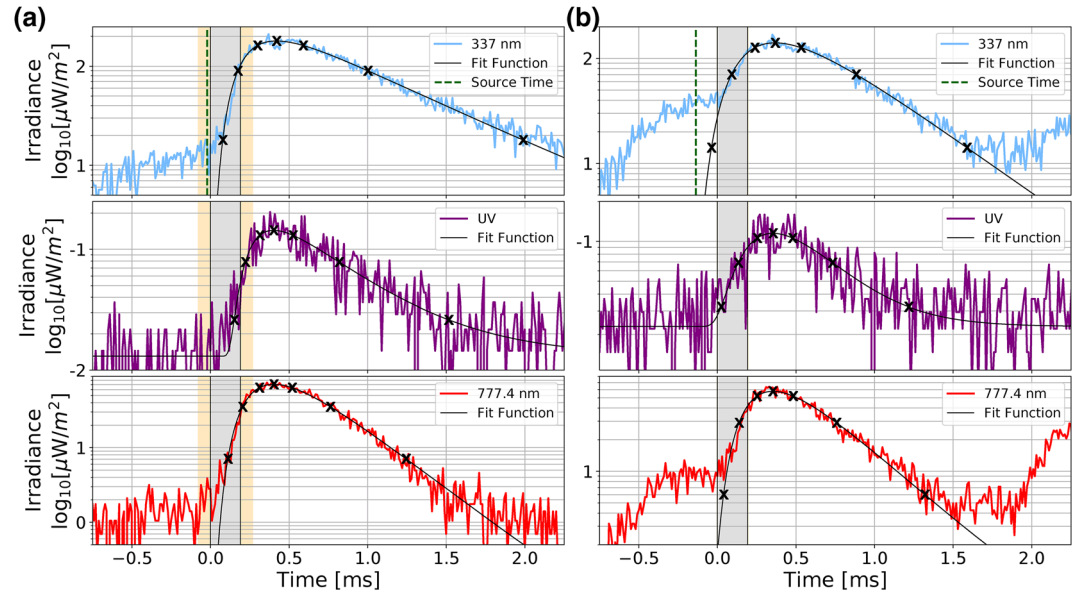


**Figure 2.** The functional fit (1) to the raw photometer signals for (a) modest prepulse activity and (b) high prepulse activity. Time  $t = 0$  is the start time of the Terrestrial Gamma-Ray Flash (TGF), the gray shaded region marks the duration of the TGF and the orange shaded region the respective time uncertainties of the measurement ( $\pm 80$  and  $\pm 5 \mu\text{s}$ ). The source time  $t_0$  (found from the fit to the first half of the pulse) is indicated with a green, dashed line in the 337 nm band, crosses mark  $f_{10}, f_{50}, f_{90}, f_{\text{max}}, f_{90t}, f_{50t}, f_{10t}$  and thus the corresponding  $t_x$  and  $t_{xt}$ .

rise time,  $t_{90} - t_{10}$ , or the duration of full width at half maximum (FWHM),  $t_{50t} - t_{50}$ ;  $t_{xt}$  denotes the times in the decaying tail of the pulse. All times  $t_x$  are relative to the first TGF photon.

To estimate the physical nature of the cloud scattering that can be derived from the function, we chose the blue band and fit only the first half of the pulse to obtain new values for  $t_0$  and  $\tau$ . This wavelength is the least affected by absorption and the first half of the pulses is from photons that have undergone the least scattering in the cloud. They are therefore the least dependent on the model assumption of an horizontally infinite cloud. In Figure 2 and the rest of this paper, given  $t_0$  and  $\tau$  refer to the values found by the latter method. A simulation model of photon scattering in arbitrary cloud geometries is described in Luque et al. (2020).

With  $\tau$ , we can estimate the depth of the optical sources inside the clouds. Therefore, we need to make assumptions regarding size distribution and density of the cloud hydrometeors. These assumptions do not impact the fitting of  $\tau$  and get important solely in estimating the depths. The depth inside the cloud depends on  $\tau$  and the diffusion coefficient  $D = \Lambda c / 3(1 - g\omega_0)$  through  $L = \sqrt{4D\tau}$  where  $\Lambda$  is the mean free path of photons,  $c$  is the speed of light,  $g$  is a wavelength dependent asymmetry factor and  $\omega_0$  is the single scattering albedo. At 337 nm,  $g \sim 0.88$  and  $\omega_0 \sim 1$ . The mean free path depends on the size,  $r_c$ , and density,  $n_c$ , distributions of cloud particles as  $\Lambda = 1 / (2\pi r_c^2 n_c)$  (Koshak et al., 1994; Light et al., 2001; Soler et al., 2020; Thomason & Krider, 1982). Thus, we estimate  $L$  based on  $\tau$  and the assumptions for  $n_c$ ,  $r_c$ ,  $g$  and  $\omega_0$ .

### 3. Results

Of the 69 TGFs selected for analysis, 62 were followed by a strong optical pulse at 337 and 777.4 nm. Equation (1) could be fitted to 52 cases out of these 62, which form the basis for the following analysis. In the UV, 14 of 52 observations have pulses that could be fitted. We do not include two simultaneous Elve detections, the luminous emissions in the ionosphere due to the excitation by strong electromagnetic pulses from lightning because of their different origin above the clouds (Neubert et al., 2020).

The results of the fits are summarized in Figure 3. The median source time  $t_0$  is  $-10 \pm 80 \mu\text{s}$  relative to the first detected photon of the TGFs with outliers up to several millisecond ( $t_0$  is only determined for the blue

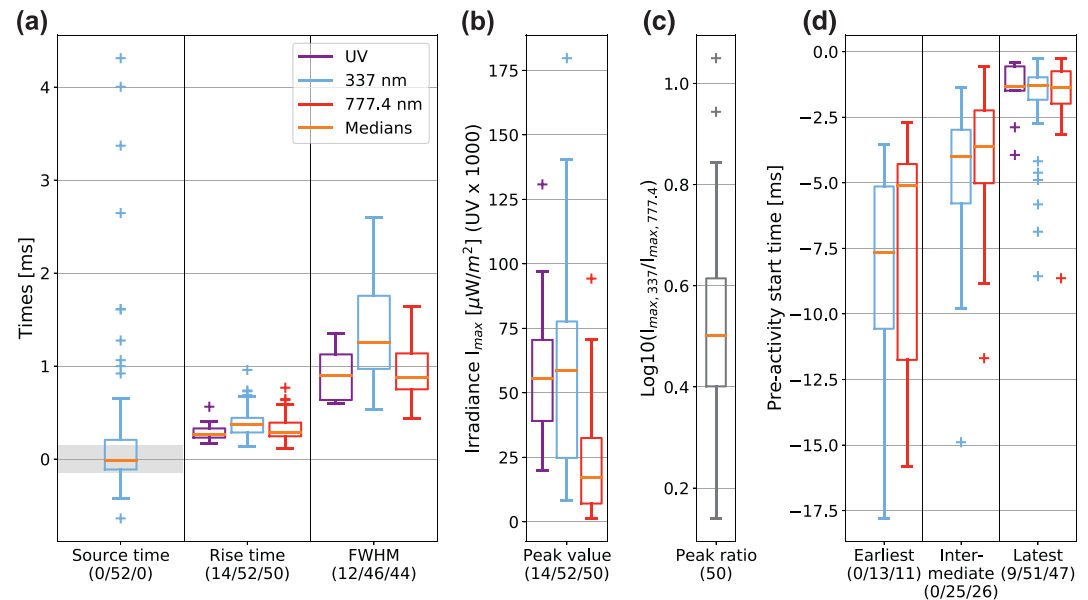


**Figure 3.** Characteristics of the optical peak following a Terrestrial Gamma-Ray Flash (TGF). The boxes represent the interquartile range of the values from the 25th to 75th percentile and the horizontal lines within are the median values. The whiskers extend to 1.5 times the interquartile range or to the maximum and minimum values if they are lower, outliers are shown as “+.” The number of observations contributing to a characteristic is given per wavelength in parenthesis below the respective label. (a) The temporal characteristics for each photometer band. From left to right, they are the source time ( $t_0$ ) relative to the arrival of the first TGF photon, the rise time, and the FWHM (full width at half maximum). The gray shaded area in the interval  $[-0.15, 0.15]$  ms indicates the uncertainty. (b) Irradiance of the optical pulses in the three bands. The irradiance in the UV band is multiplied by 1,000 to show it on the same scale as the other bands. (c) Ratio of the peak values of 337 and 777 nm. (d) Start of the preactivity for the cases of 3, two and one pulse(s) prior to start of the main pulse, the order is explained in the text.

signal). The rise times are  $\sim 260\text{--}370$   $\mu\text{s}$  and the FWHM is around 1 ms. The FWHM is larger for 337 nm than for 777.4 nm, consistent with more scattering of blue photons and higher absorption of red photons. Compared to statistics of lighting flashes without identified TGFs (Christian & Goodman, 1987; Offroy et al., 2015), the pulses presented here exhibit slightly longer rise times,  $+50\text{--}100$   $\mu\text{s}$ , and doubled FWHMs,  $\sim 1\text{--}1.5$  ms. The time parameters of UV emissions are more similar to the red than to the blue, but suffer generally most from atmospheric absorption (Luque et al., 2020; Molina & Molina, 1986). Neither rise time nor FWHM are affected by the instrumental timing uncertainty. Two observations in the red band could not be used for the statistics and six observations showed secondary peaks starting before  $t_{0t}$  of the main peak, so we did not take them into account for the FWHM. More values are given in the supplement.

The majority of the source times is within the instrumental and model uncertainties of the TGF start, for example, Figure 2a. We conclude, then, that the majority of optical pulses are emitted at the onset of TGFs, consistent with previous case studies (Alnussirat et al., 2019; Neubert et al., 2020; Østgaard et al., 2019b), with some cases delayed up to  $\sim 4$  ms. The uncertainties are discussed further in the next section. The optical source duration is modeled by a function that describes an instantaneous source, suggesting that the pulse duration may be caused by cloud scattering, just as TGF pulses are broadened by Compton scattering (Cestlin & Pasko, 2012). Both sources, optical and gamma ray, are then presumably of comparable duration.

The peak irradiance in the blue is generally  $\sim 3$  times stronger than in the red (Figures 3b and 3c), while 777.4 nm emissions dominate regular lightning pulses, that is, ratios  $\leq 1$  (e.g., Adachi et al., 2016). For the cases with UV pulses, the amplitudes of the blue and the UV correlate with a magnitude difference of  $10^3$ .

During the preactivity, the red and blue photometer signals show 1–3 pulses of increasing signal amplitude when approaching the onset of the main optical pulse. All but one observation have at least one preactivity pulse, half the observations have two pulses and a quarter have three pulses. In the UV band, nine observations had one preceding pulse, more than one was not observed. The event without preactivity is of low

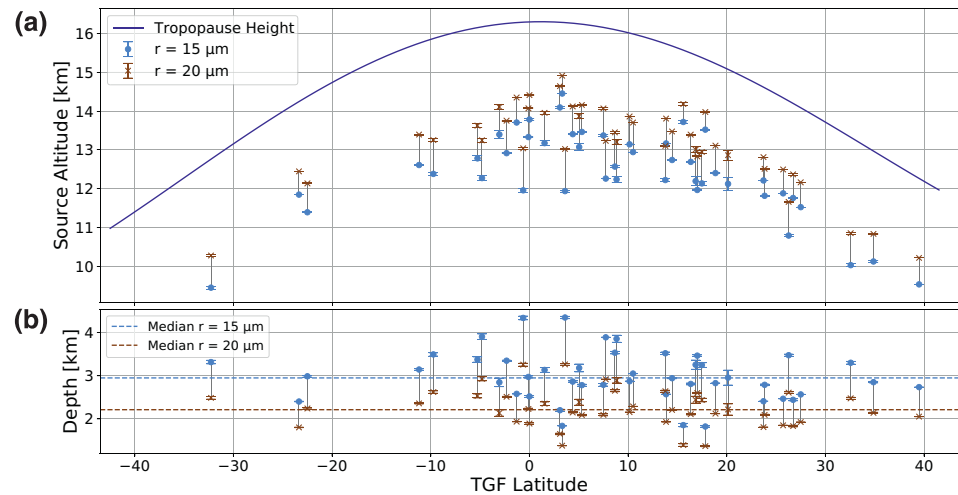


**Figure 4.** Estimated source altitudes (a) and depths inside clouds (b) of the optical pulses associated with Terrestrial Gamma-Ray Flashes for  $n_c = 2.5 \times 10^8 \text{ m}^{-3}$ .

overall intensity, suggesting it was undetected. The statistics of preactivity pulse start times in Figure 3d is sorted by the temporal proximity of the pulses to the main optical pulse. In the cases with only one pulse, this pulse is part of “latest.” For two pulses, the earlier pulse is taken as “intermediate,” the latter as “latest.” For three pulses, the first one is in “earliest,” the second in “intermediate,” and the third in “latest.” The intervals between the pulses shorten when approaching the main peak. Optical emissions more than 20 ms prior to the TGF from the same location were observed in 2 of the 52 cases (not shown). In both of them, the detections were of low intensity and dominantly blue, consistent with the the rest of the preactivity measurements. Consequently, TGFs occur in the initial phase of a flash without extensive optical activity before them. Intensities and durations of the preactivity pulses are summarized in the supplement.

The depth in the clouds of the optical sources at TGF onset were estimated from the fit of the first half of the blue photometer signal as described earlier. We assume a cloud top composition of water ice droplets with typical values  $r_c = 15, 20 \mu\text{m}$  and  $n_c = 2.5 \times 10^8 \text{ m}^{-3}$  (Dye et al., 2007; Ursi et al., 2019) while also accounting for the direction from the source to the detector relative to zenith. The altitude is estimated by assuming the cloud tops are at the tropopause (Splitt et al., 2010; Ursi et al., 2019) and that the tropopause altitude follows equation (2) of Offroy et al. (2015).

The result is shown in Figure 4. The optical sources that can be approximated by the fit function (52 of 69 events) are in the top of the cloud and at a few km depth, consistent with Stanley et al. (2006); Cummer et al. (2015). The depth and altitude depend on the parameter values that enter the assumptions on the cloud particles, where less dense clouds,  $r_c = 15 \mu\text{m}$ , lead to greater depths. For  $n_c = 10^8 \text{ m}^{-3}$ , the altitudes are 1–2 km lower. The choice of  $r_c$  and  $n_c$  accounts for the biggest uncertainties, while the errors on  $\tau$  are small. Besides uncertainties, Brunner and Bitzer (2020) showed the influence of different cloud compositions and source depths on the amount of optical emissions exiting the cloud top.

We conclude this section by noting a simple method to estimate the parameter  $\tau$ , which is the only pulse parameter entering the altitude estimation. We find it can be approximated from the FWHM as  $\tau = k \times FWHM + d$  with  $k = 0.853 \pm 0.29$  and  $d = -0.001 \pm 0.429$ , see also Figure S4 in the supplement.

#### 4. Discussion and Interpretation

Upward negative intracloud leaders in the upper cloud regions are thought to create a conducting connection between the central negative charge region toward the upper positive charge region while producing 1–3 bursts of initial breakdown pulses (IBPs) with 1–5 ms between the bursts. IBPs are signatures in signals measured by electric field sensors (Marshall et al., 2013). Video recordings from the ground show luminosity

increases in the visible spectrum at the time of large IBPs (Stolzenburg et al., 2016). The observation of 1–3 preactivity pulses with increasing intensity observed by ASIM agrees then well with upward propagating leaders that produce luminous IBP bursts (cf. Figure S2) and are further evidence of TGFs occurring at the onset of flashes. Shorter intervals of the pulses (Figure 3d) further suggest an upward acceleration of the leaders as discussed by Cummer et al. (2015).

Some TGFs are connected with so-called energetic in-cloud pulses (EIPs) observed by ground networks in low frequency (LF) signals (30–300 kHz). EIPs are associated with large currents and are typically detected 1–3 ms after the initiation of upward negative leaders in the upper regions of the clouds (Lyu et al., 2015, 2016). The TGFs we report in this study are related to significant leader current surges, that is, red peaks (e.g., Bitzer et al., 2016), and their estimated source altitudes are likewise in the upper regions of the clouds (Figure 4). This opens the question if our optical main peaks are manifestations of EIPs. Whereas only 12% of TGFs are associated with EIPs (Lyu et al., 2016), we find that almost all of them are followed by strong optical pulses and some with preactivity starting many millisecond earlier (Figure 3d). The pulses have a higher blue-to-red ratio (Figure 3c) and longer durations than lightning without identified TGFs (Adachi et al., 2016; Christian & Goodman, 1987; Offroy et al., 2015), suggesting that they are a special type of current surge. While events with only one preactivity pulse seem consistent with reported EIP sequences, also other LF signals are reported in association with TGFs in similar altitudes, such as “slow pulses” (Pu et al., 2019). It remains to be explained how the different LF signatures relate to the optical detections.

The optical scattering properties of the cloud, estimated from Equation 1, must be taken with caution since lightning is spatially and temporally extended. However, as long as the source onset is short compared to the rise times of the optical pulses, that is, less than  $\sim 100 \mu\text{s}$ , we find the fit function to the first half of the pulse, from which we estimate  $t_0$  and  $\tau$ , to be relatively insensitive to the assumption on the temporal variation of the source. Nevertheless, the source duration is likely much shorter than the measured pulse durations and likely in the range of TGF sources, which are typically a few 100  $\mu\text{s}$  or less (Marisaldi et al., 2014; Østgaard et al., 2019b). As in scattering of optical emissions, TGFs are broadened by Compton scattering (Celestin & Pasko, 2012), indicating that the sources are a few tens of microsecond in duration. The average duration of LF waveforms is 55  $\mu\text{s}$  for EIPs (Lyu et al., 2015) and  $\sim 80 \mu\text{s}$  for slow pulses (Pu et al., 2019). Consequently, all inferred source durations related to TGF detection (LF, optical, TGF photons) are down to  $\sim 10\text{s}$  to few 100s of  $\mu\text{s}$ .

To investigate the accuracy of  $t_0$ , we derived  $t_0$  from the red signal (leader emissions) and compared it to the start times of UV signatures of two cases with simultaneous Elves (powered by electromagnetic pulses from impulsive leader currents). We find  $t_{0,red}$  to be  $59 \pm 8$  and  $22 \pm 7 \mu\text{s}$  before the onset of the Elve emissions in the UV, while  $t_{0,blue}$  was  $113 \pm 6$  and  $99 \pm 8 \mu\text{s}$  earlier. Since Elve emissions are unaffected by cloud scattering, they are an estimate of the onset time of the current pulses. Elves are expanding rings in the lower ionosphere extending hundreds of km in horizontal radius. The detection of their onset is typically  $\sim 20 \mu\text{s}$  delayed due to the geometry and lifetime of the emissions relative to the sensors. Accounting for this delay,  $t_{0,red}$  is  $\sim 40$  and  $\sim 0 \mu\text{s}$  before the Elve. However, this example also shows how the preactivity interferes with the fitting procedure on this precise level: The Elve case with a 777-UV delay of  $22/\sim 0 \mu\text{s}$  has a preactivity intensity of  $<5\%$ , while the maximum preactivity intensity was  $\sim 30\%$  in the case with the larger delay ( $\sim 60/40 \mu\text{s}$ ). Therefore, we have to assume that preactivity levels above  $\sim 20\%$  of the main pulse intensity introduce methodical uncertainties of up to  $\sim 30\text{--}40 \mu\text{s}$ , valid also for the blue activity and the respective  $t_0$  values. Additional uncertainty is possibly introduced by Elve emissions in the blue band. From the cases studied, we expect intensities less than those in the UV,  $\sim 3\text{--}4 \mu\text{W}/\text{m}^2$ , which are of the order of, or smaller than, the preactivity. The analysis of the two Elves indicates the mutual production of the red leader emissions and the Elves, while the blue emissions appear to start before this phase.

With the instrumental and methodical uncertainties,  $\pm 80$  or  $\pm 5 \mu\text{s}$  as mentioned earlier and  $\sim 30\text{--}40 \mu\text{s}$ , respectively, the median source time of the optical pulses at  $-10 \mu\text{s}$  before the TGF onset (Figure 3a) is smaller than the accuracy of the source time identification and does not allow to address the sequence of the events. For outliers more than  $\sim 150 \mu\text{s}$  before or after the TGF onset, the sequence seems to be clear, provided we have identified the correct pulse associations with the TGF.

The consistent occurrence of optical signals in the blue (337 nm) and red (777.4 nm) bands for all TGFs connects the production of TGFs to streamer and leader processes. Leaders emit dominantly in the red band, while their blue emissions are 30–40 times lower (Armstrong et al., 1998; Nijdam, 2011, Chapter 8). Streamers emit dominantly in the blue band with neglectable amounts of radiation in the 777.4 nm band (Ebert et al., 2010; Nijdam, 2011, Chapter 8). Consequently, we attribute the majority of blue emissions in our detections (Figures 3b and 3c) to high levels of streamer activity. Combined with measurements of VHF (30–300 MHz) activity related to TGFs by others, proposed to be a signature of temporally and spatially extended source regions (Lyu et al., 2018), we suggest a scenario where the optical and TGF emissions are generated as the atmosphere of the region ahead of the leader tip breaks down in a flash of streamers, high-energy electrons and a leader current surge (Köhn et al., 2020). Optical detections after the main peak, observed for many events (Figures 1c and 1e), are likely continued leader activity and branching in the cloud (Cummer et al., 2015). The pulse durations and rise times together with the estimated altitudes do not suggest detection of optical emission due to TGF excitation from above the cloud Xu et al. (2017).

### Data and Materials Availability Statement

ASIM data and Vaisala GLD360 detections are available via [asdc.space.dtu.dk](https://asdc.space.dtu.dk). ISS-LIS data is available from Blakeslee (2019). The data used to generate the figures are available from the data repository with doi: 10.5281/zenodo.4279394.

### Acknowledgments

MH appreciates discussions with and feedback from Joe Dwyer. The authors thank two anonymous reviewers for their useful suggestions and feedback which helped to improve the paper. The authors thank VAISALA for the GLD360 lightning data. ASIM is a mission of the European Space Agency (ESA) and is funded by ESA and by national grants of Denmark, Norway and Spain. The ASIM Science Data Center is supported by ESA PRODEX contracts C 4000115884 (DTU) and 4000123438 (Bergen). The science analysis is supported by: the European Research Council grant n. 320839, the Research Council of Norway contracts 223252/F50 (CoE/BCSS), the Ministerio Ciencia e Innovacion grant ESP 2017-86263-C4, and project grant PID2019-109269RB. This project has received funding from the European Union's Horizon 2020 research and innovation program under the Marie Skłodowska-Curie grant agreement 722337. FJPI acknowledges the sponsorship provided by the Federal Ministry for Education and Research of Germany through the Alexander von Humboldt Foundation.

### References

- Adachi, T., Sato, M., Ushio, T., Yamazaki, A., Suzuki, M., Kikuchi, M., et al. (2016). Identifying the occurrence of lightning and transient luminous events by nadir spectrophotometric observation. *Journal of Atmospheric and Solar-Terrestrial Physics*, 145, 85–97. <https://doi.org/10.1016/j.jastp.2016.04.010> Retrieved from <https://linkinghub.elsevier.com/retrieve/pii/S1364682616301109>
- Alnussirat, S. T., Christian, H. J., Fishman, G. J., Burchfield, J., & Cherry, M. L. (2019). Simultaneous space-based observations of terrestrial gamma-ray flashes and lightning optical emissions: Investigation of the terrestrial gamma-ray flash production mechanisms. *Physical Review D*, 100(8), 083018. <http://dx.doi.org/10.1103/physrevd.100.083018>
- Armstrong, R., Shorter, J., Taylor, M., Suszcynsky, D., Lyons, W., & Jeong, L. (1998). Photometric measurements in the SPRITES '95 & '96 campaigns of nitrogen second positive (399.8 nm) and first negative (427.8 nm) emissions. *Journal of Atmospheric and Solar-Terrestrial Physics*, 60(7–9), 787–799. [https://doi.org/10.1016/S1364-6826\(98\)00026-1](https://doi.org/10.1016/S1364-6826(98)00026-1)
- Bitzer, P. M., Burchfield, J. C., & Christian, H. J. (2016). A Bayesian Approach to Assess the Performance of Lightning Detection Systems. *Journal of Atmospheric and Oceanic Technology*, 33(3), 563–578. <https://doi.org/10.1175/JTECH-D-15-0032.1>
- Blakeslee, R. J. (2019). *Non-quality controlled lightning imaging sensor (LIS) on international space station (ISS) science data*. Huntsville, AL, U.S.A: NASA Global Hydrology Resource Center DAAC. Retrieved from [https://ghrc.nsstc.nasa.gov/hydro/details/isslis\\_v1\\_nqc](https://ghrc.nsstc.nasa.gov/hydro/details/isslis_v1_nqc), <https://doi.org/10.5067/LIS/ISSLIS/DATA107>
- Blakeslee, R. J., Lang, T. J., Koshak, W. J., Buechler, D., Gatlin, P., Mach, D. M., et al. (2020). Three years of the lightning imaging sensor onboard the international space station: Expanded global coverage and enhanced applications. *Journal of Geophysical Research: Atmospheres*, 125(16), 1–20. <https://doi.org/10.1029/2020JD032918>
- Brunner, K. N., & Bitzer, P. M. (2020). A first look at cloud inhomogeneity and its effect on lightning optical emission. *Geophysical Research Letters*, 47(10), 1–9. <https://doi.org/10.1029/2020GL087094>
- Celestin, S., & Pasko, V. P. (2011). Energy and fluxes of thermal runaway electrons produced by exponential growth of streamers during the stepping of lightning leaders and in transient luminous events. *Journal of Geophysical Research*, 116(A03315), 1–14. <https://doi.org/10.1029/2010JA016260>
- Celestin, S., & Pasko, V. P. (2012). Compton scattering effects on the duration of terrestrial gamma-ray flashes. *Geophysical Research Letters*, 39(L02802), 1–4. <https://doi.org/10.1029/2011GL050342>
- Chanrion, O., Bonaventura, Z., Çinar, D., Bourdon, A., & Neubert, T. (2014). Runaway electrons from a 'beam-bulk' model of streamer: application to TGFs. *Environmental Research Letters*, 9(055003), 1–9. <https://doi.org/10.1088/1748-9326/9/5/055003>
- Chanrion, O., Neubert, T., Lundgaard Rasmussen, I., Stoltze, C., Tcherniak, D., Jessen, N. C., et al. (2019). The Modular Multispectral Imaging Array (MMIA) of the ASIM payload on the international space station. *Space Science Reviews*, 215(28), 1–25. <https://doi.org/10.1007/s11214-019-0593-y>
- Christian, H. J., & Goodman, S. J. (1987). Optical observations of lightning from a high-altitude airplane. *Journal of Atmospheric and Oceanic Technology*, 4(4), 701–711. [https://doi.org/10.1175/1520-0426\(1987\)004<0701:OOOLFA>2.0.CO;2](https://doi.org/10.1175/1520-0426(1987)004<0701:OOOLFA>2.0.CO;2)
- Cummer, S. A., Lyu, F., Briggs, M. S., Fitzpatrick, G., Roberts, O. J., & Dwyer, J. R. (2015). Lightning leader altitude progression in terrestrial gamma-ray flashes. *Geophysical Research Letters*, 42(18), 7792–7798. <https://doi.org/10.1002/2015GL065228>
- da Silva, C. L., & Pasko, V. P. (2013). Dynamics of streamer-to-leader transition at reduced air densities and its implications for propagation of lightning leaders and gigantic jets. *Journal of Geophysical Research: Atmospheres*, 118(24), 13561–13590. <https://doi.org/10.1002/2013JD020618>
- Dwyer, J. R. (2008). Source mechanisms of terrestrial gamma-ray flashes. *Journal of Geophysical Research*, 113(D10103), 1–12. <https://doi.org/10.1029/2007JD009248>
- Dye, J. E., Bateman, M. G., Christian, H. J., Defer, E., Grainger, C. A., Hall, W. D., et al. (2007). Electric fields, cloud microphysics, and reflectivity in anvils of Florida thunderstorms. *Journal of Geophysical Research*, 112(D11215), 1–18. <https://doi.org/10.1029/2006JD007550>

- Ebert, U., Nijdam, S., Li, C., Luque, A., Briels, T., & van Veldhuizen, E. (2010). Review of recent results on streamer discharges and discussion of their relevance for sprites and lightning. *Journal of Geophysical Research*, *115*(A00E43), 1–13. <https://doi.org/10.1029/2009JA014867>
- Fishman, G. J., Bhat, P. N., Mallozzi, R., Horack, J. M., Koshut, T., Kouveliotou, C., et al. (1994). Discovery of intense gamma-ray flashes of atmospheric origin. *Science*, *264*(5163), 1313–1316. <https://doi.org/10.1126/science.264.5163.1313>
- Gjesteland, T., Østgaard, N., Bitzer, P., & Christian, H. J. (2017). On the timing between terrestrial gamma ray flashes, radio atmospheric, and optical lightning emission. *Journal of Geophysical Research: Space Physics*, *122*(7), 7734–7741. <https://doi.org/10.1002/2017JA024285>
- Gurevich, A., Milikh, G., & Roussel-Dupre, R. (1992). Runaway electron mechanism of air breakdown and preconditioning during a thunderstorm. *Physics Letters A*, *165*(5–6), 463–468. [https://doi.org/10.1016/0375-9601\(92\)90348-P](https://doi.org/10.1016/0375-9601(92)90348-P)
- Köhn, C., Diniz, G., & Haraheh, M. N. (2017). Production mechanisms of leptons, photons, and hadrons and their possible feedback close to lightning leaders. *Journal of Geophysical Research*, *122*(2), 1365–1383. <https://doi.org/10.1002/2016JD025445>
- Köhn, C., & Ebert, U. (2015). Calculation of beams of positrons, neutrons, and protons associated with terrestrial gamma ray flashes. *Journal of Geophysical Research: Atmospheres*, *120*(4), 1620–1635. <https://doi.org/10.1002/2014JD022229>
- Köhn, C., Heumesser, M., Chanrion, O., Nishikawa, K., Reglero, V., & Neubert, T. (2020). The emission of terrestrial gamma ray flashes from encountering streamer coronae associated to the breakdown of lightning leaders. *Geophysical Research Letters*, *47*(20), 1–11. <https://doi.org/10.1029/2020GL089749>
- Koshak, W. J., Solakiewicz, R. J., Phanord, D. D., & Blakeslee, R. J. (1994). Diffusion model for lightning radiative transfer. *Journal of Geophysical Research*, *99*(D7), 14361–14371. <https://doi.org/10.1029/94JD00022>
- Light, T. E., Suszcynsky, D. M., Kirkland, M. W., & Jacobson, A. R. (2001). Simulations of lightning optical waveforms as seen through clouds by satellites. *Journal of Geophysical Research*, *106*(D15), 17103–17114. <https://doi.org/10.1029/2001JD900051>
- Luque, A., Gordillo-Vázquez, F. J., Li, D., Malagón-Romero, A., Pérez-Invernón, F. J., Schmalzried, A., et al. (2020). Modeling lightning observations from space-based platforms (CloudScatJl 1.0). *Geoscientific Model Development*, *13*(11), 5549–5566. <http://dx.doi.org/10.5194/gmd-13-5549-2020>
- Lyu, F., Cummer, S. A., Briggs, M., Marisaldi, M., Blakeslee, R. J., Bruning, E., et al. (2016). Ground detection of terrestrial gamma ray flashes from distant radio signals. *Geophysical Research Letters*, *43*(16), 8728–8734. <https://doi.org/10.1002/2016GL070154>
- Lyu, F., Cummer, S. A., Krehbiel, P. R., Rison, W., Briggs, M. S., Cramer, E., et al. (2018). Very high frequency radio emissions associated with the production of terrestrial gamma-ray flashes. *Geophysical Research Letters*, *45*(4), 2097–2105. <https://doi.org/10.1002/2018GL077102>
- Lyu, F., Cummer, S. A., & McTague, L. (2015). Insights into high peak current in cloud lightning events during thunderstorms. *Geophysical Research Letters*, *42*(16), 6836–6843. <https://doi.org/10.1002/2015GL065047>
- Marisaldi, M., Fuschino, F., Tavani, M., Dietrich, S., Price, C., Galli, M., et al. (2014). Properties of terrestrial gamma ray flashes detected by AGILE MCAL below 30 MeV. *Journal of Geophysical Research: Space Physics*, *119*(2), 1337–1355. <https://doi.org/10.1002/2013JA019301>
- Marisaldi, M., Galli, M., Labanti, C., Østgaard, N., Sarria, D., Cummer, S. A., et al. (2019). On the high energy spectral component and fine time structure of terrestrial gamma ray flashes. *Journal of Geophysical Research: Atmospheres*, *124*(14), 7484–7497. <https://doi.org/10.1029/2019JD030554>
- Marshall, T., Stolzenburg, M., Karunarathne, S., Cummer, S., Lu, G., Betz, H.-D., & Xiong, S. (2013). Initial breakdown pulses in intracloud lightning flashes and their relation to terrestrial gamma ray flashes. *Journal of Geophysical Research: Atmospheres*, *118*(19), 10907–10925. <https://doi.org/10.1002/jgrd.50866>
- Molina, L. T., & Molina, M. J. (1986). Absolute absorption cross sections of ozone in the 185- to 350-nm wavelength range. *Journal of Geophysical Research*, *91*(D13), 14501–14508. <https://doi.org/10.1029/JD091iD13p14501>
- Moss, G. D., Pasko, V. P., Liu, N., & Veronis, G. (2006). Monte Carlo model for analysis of thermal runaway electrons in streamer tips in transient luminous events and streamer zones of lightning leaders. *Journal of Geophysical Research*, *111*(A02307), 1–37. <https://doi.org/10.1029/2005JA011350>
- Neubert, T., Østgaard, N., Reglero, V., Blanc, E., Chanrion, O., Oxborrow, C. A., et al. (2019). The ASIM mission on the international space station. *Space Science Reviews*, *215*(26), 1–17. <https://doi.org/10.1007/s11214-019-0592-z>
- Neubert, T., Østgaard, N., Reglero, V., Chanrion, O., Heumesser, M., Dimitriadou, K., et al. (2020). A terrestrial gamma-ray flash and ionospheric ultraviolet emissions powered by lightning. *Science*, *367*(6474), 183–186. <https://doi.org/10.1126/science.aax3872> Retrieved from <https://science.sciencemag.org/content/367/6474/183>
- Nijdam, S. (2011). *Experimental investigations on the physics of streamers [PhD]*. Eindhoven: Technische Universiteit Eindhoven. Retrieved from <http://alexandria.tue.nl/extra2/693618.pdf>
- Offroy, M., Farges, T., Kuo, C. L., Chen, A. B. C., Hsu, R. R., Su, H. T., et al. (2015). Temporal and radiometric statistics on lightning flashes observed from space with the ISUAL spectrophotometer. *Journal of Geophysical Research*, *120*(15), 7586–7598. <https://doi.org/10.1002/2015JD023263>
- Østgaard, N., Balling, J. E., Bjørnsen, T., Brauer, P., Budtz-Jørgensen, C., Bujwan, W., & Yang, S. (2019a). The Modular X- and Gamma-Ray Sensor (MXGS) of the ASIM payload on the international space station. *Space Science Reviews*, *215*(23), 1–28. <https://doi.org/10.1007/s11214-018-0573-7>
- Østgaard, N., Gjesteland, T., Carlson, B. E., Collier, A. B., Cummer, S. A., Lu, G., & Christian, H. J. (2013). Simultaneous observations of optical lightning and terrestrial gamma ray flash from space. *Geophysical Research Letters*, *40*(10), 2423–2426. <https://doi.org/10.1002/grl.50466>
- Østgaard, N., Neubert, T., Reglero, V., Ullaland, K., Yang, S., Genov, G., et al. (2019b). First 10 months of TGF observations by ASIM. *Journal of Geophysical Research: Atmospheres*, *124*(24), 14024–14036. <https://doi.org/10.1029/2019JD031214>
- Pu, Y., Cummer, S. A., Lyu, F., Briggs, M., Mailyan, B., Stanbro, M., & Roberts, O. (2019). Low frequency radio pulses produced by terrestrial gamma ray flashes. *Geophysical Research Letters*, *46*(12), 6990–6997. <https://doi.org/10.1029/2019GL082743>
- Soler, S., Pérez Invernón, F. J., Gordillo Vázquez, F. J., Luque, A., Li, D., Malagón Romero, A., et al. (2020). Blue optical observations of narrow bipolar events by ASIM suggest corona streamer activity in thunderstorms. *Journal of Geophysical Research: Atmospheres*, *125*(16), 1–13. <https://doi.org/10.1029/2020JD032708>
- Splitt, M. E., Lazarus, S. M., Barnes, D., Dwyer, J. R., Rassoul, H. K., Smith, D. M., et al. (2010). Thunderstorm characteristics associated with RHESSI identified terrestrial gamma ray flashes. *Journal of Geophysical Research*, *115*(A00E38), 1–10. <https://doi.org/10.1029/2009JA014622>
- Stanley, M. A., Shao, X.-M., Smith, D. M., Lopez, L. I., Pongratz, M. B., Harlin, J. D., et al. (2006). A link between terrestrial gamma-ray flashes and intracloud lightning discharges. *Geophysical Research Letters*, *33*(L06803), 1–5. <https://doi.org/10.1029/2005GL025537>
- Stolzenburg, M., Marshall, T. C., Karunarathne, S., & Orville, R. E. (2016). Luminosity with intracloud-type lightning initial breakdown pulses and terrestrial gamma-ray flash candidates. *Journal of Geophysical Research: Atmospheres*, *121*(18), 10919–10936. <https://doi.org/10.1002/2016JD025202>

- Thomason, L. W., & Krider, E. P. (1982). The effects of clouds on the light produced by lightning. *Journal of the Atmospheric Sciences*, 39(9), 2051–2065. [https://doi.org/10.1175/1520-0469\(1982\)039<2051:TEOCOT>2.0.CO;2](https://doi.org/10.1175/1520-0469(1982)039<2051:TEOCOT>2.0.CO;2)
- Ursi, A., Marisaldi, M., Dietrich, S., Tavani, M., Tiberia, A., & Porcù, F. (2019). Analysis of thunderstorms producing terrestrial gamma ray flashes with the meteosat second generation. *Journal of Geophysical Research: Atmospheres*, 124(23), 12667–12682. <https://doi.org/10.1029/2018JD030149>
- Wilson, C. T. R. (1925). The electric field of a thunderstorm and some of its effects. *Proceedings of the Royal Society of London*, 37(32D), 32D–37D. <https://doi.org/10.1088/1478-7814/37/1/314>
- Xu, W., Celestin, S., & Pasko, V. P. (2012). Source altitudes of terrestrial gamma-ray flashes produced by lightning leaders. *Geophysical Research Letters*, 39(L08801), 1–5. <https://doi.org/10.1029/2012GL051351>
- Xu, W., Celestin, S., & Pasko, V. P. (2015). Optical emissions associated with terrestrial gamma ray flashes. *Journal of Geophysical Research: Space Physics*, 120(2), 1355–1370. <https://doi.org/10.1002/2014JA020425>
- Xu, W., Celestin, S., Pasko, V. P., & Marshall, R. A. (2017). A novel type of transient luminous event produced by terrestrial gamma-ray flashes. *Geophysical Research Letters*, 44(5), 2571–2578. <https://doi.org/10.1002/2016GL072400>